PCCP

Accepted Manuscript

ROYAL SOCIETY OF CHEMISTRY

www.rsc.org/pccp

Journal Name

ARTICLE

Dynamic Conjugated Microporous Polymers: Visible Light-Harvesting via Guest Responsive Reversible Swelling

Received 00th January 20xx,
Accepted 00th January 20xx

DOI: 10.1039/x0xx00000x

www.rsc.org/

K. Venkata Rao,[a] Ritesh Haldar,[a] Tapas Kumar Maji,[a,b]* and Subi J. George[a]*

The Light-harvesting properties of two fluorescent dynamic conjugated microporous organic polymers (**Py-PP** and **Py-BPP**) rendered with pyrene chromophores are described. The hydrophobic and dynamic nature of these porous frameworks allows the selective capture of various organic solvents by the instantaneous swelling at room temperature. Moreover the dynamic nature of these frameworks indicates the swelling process with visible volume expansion and enhanced fluorescence. This was further explored for the rapid encapsulation of various fluorescent chromophoric guests at room temperature and investigated for photoinduced energy transfer process. The resultant host-guest antenna materials showed efficient light-harvesting and funnelling of excitation energy of host framework towards the entrapped guest molecule. This process further yielded solid-state luminescent materials with tunable emission. This work holds a great promise on the design of smart porous organic solids from π-conjugated small molecules for optoelectronics, sensing and separation.

INRODUCTION

Much attention has been devoted in recent years for the design of synthetic host materials that can capture and entrap guest molecules with specific host-guest interactions.[1–3] It has been shown that the host materials can alter the physical and chemical properties of the guest molecules there by giving room for new phenomenon within their confined cavities.[4,5] These strategies are technologically important for sensing, catalysis, separation and purification of specific targets. In this context, discrete molecular hosts such as calixarenes,[6] molecular capsules[7] and metal-organic cages[8] were exploited for various applications. Interestingly, the discovery of extended porous materials such as crystalline molecular flasks,[9] metal-organic frameworks (MOFs)[10,11] and periodic mesoporous organosilica (PMO)[12–14] having extended 3D cavities has brought many advances in this field with improved functions compared to discrete molecular cages. However, these porous framework materials are not ideal candidates for rapid and reversible capture of organic solvents and guest molecules due to their rigid structure and poor chemical and hydrothermal stability.[15,16] Moreover, encapsulation of appropriate guest molecules in these rigid host frameworks often requires harsh and lengthy procedures.[17] In this context, porous organic polymers (POPs)[18–24] synthesized from pure organic linkers would be promising owing to their high thermal and chemical stability and tunable surface areas.[25–27] However, most of the POPs reported so far contain non-dynamic backbones and hardly show any guest encapsulation properties. We envisage that, imparting dynamic functionality into these robust materials would enable their guest encapsulation properties and hence can be exploited in wide range of applications. In this regard, dynamic soft porous MOF developed by Kitagawa et al. is an impressive example.[28,29] These dynamic MOFs serve as excellent gas sensors even under low pressures of analyte molecules.[30] We have recently observed that POPs derived from pyrene chromophores (**Py-PP**) pose dynamic framework.[31] Owing to the porous dynamic backbone, **Py-PP** showed multifunctional behaviour such as guest-responsive reversible swelling, enhanced fluorescence and super-absorbent nature in organic solvents which are previously unknown for POPs. Recently similar design principles have been applied to various POPs and exploited for sensing[32,33] and photocatalysis.[34] Moreover, strong visible light absorption, luminescence and good wettability with various organic solvents of **Py-PP** make it as a potential material for the production of H_2 gas from water under visible light.[34]

On the other hand, design of artificial light-harvesting materials[35–43] is a meticulous area of research as they are key ingredients in advanced photovoltaic and optoelectronic devices. Light-harvesting and energy-transfer processes were extensively investigated in porous materials such as MOFs[44–50] and PMOs[38,51] in the context of tunable luminescence and photocatalysis. However, encapsulation of acceptor guest (luminescent trap) in these porous materials is challenging. It

[a] Supramolecular Chemistry Laboratory, New Chemistry Unit, Jawaharlal Nehru Centre for Advanced Scientific Research (JNCASR), Jakkur P.O, Bangalore 560064, India. E-mail : george@jncasr.ac.in; Fax: + 91 80 22082760; Tel: + 9 1 8 0 2 2 0 8 2 9 6 4
[b] Chemistry and Physics of Materials Unit, Jawaharlal Nehru Centre for Advanced Scientific Research (JNCASR), Jakkur P.O, Bangalore 560064, India.
E-mail: tmaji@jncasr.ac.in.

Electronic Supplementary Information (ESI) available: Supporting figures. See DOI: 10.1039/x0xx00000x

has been shown that conjugated luminescent POPs can serve as versatile donor scaffolds for excitation energy-transfer due to efficient exciton migration along conjugated backbones.[52–54] Till to date very few conjugated POPs are exploited for energy-transfer process mainly due to their non-dynamic and poor guest encapsulation properties. Now it is highly reasonable to use luminescent, dynamic and superabsorbent POPs as novel class of donor scaffolds for excitation energy-transfer because, they facilitate easy and quick encapsulation of acceptor dye molecules under ambient conditions. Moreover, apart from gas storage and catalysis,[55] functional properties that are characteristics of POPs made from π-conjugated back bones such as luminescence[56,57] and energy-transfer are seldom reported.

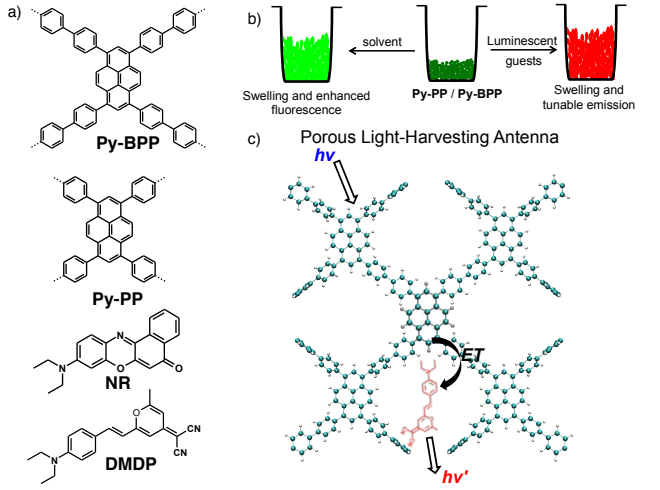

Scheme 1 (a) Molecular structures of microporous polymers (**Py-PP** and **Py-BPP**) and guest molecules (**DMDP** and **NR**). (b) Schematic of solvent induced swelling and facile guest encapsulation into dynamic porous poymer frameworks. (c) Schematic representation of light-harvesting process from porous poymer framework to the entrapped chromophores.

Here we describe the light-harvesting properties of two dynamic microporous polymer networks (**Py-PP** and **Py-BPP**) rendered with green fluorescent pyrene scaffold (Scheme 1). The unique swelling and dynamic nature of these polymers in various organic solvents enabled a facile, room temperature encapsulation of red emitting 4-(Dicyanomethylene)-2-methyl-6-(4-dimethylaminostyryl)-4*H*-pyran (**DMDP**) and nile red (**NR**) dyes (Scheme 1b). The resulting host-guest antenna materials showed efficient light-harvesting and tunable solid-state emission (Scheme 1c).[58] The ability of these polymers to absorb wide range of guest molecules ranging from small solvent molecules to big organic dyes reiterates the importance of dynamic porous materials as they can undergo structural reorganization in response to incoming guest molecules.

EXPERIMENTAL SECTION

General methods:

Electronic emission spectra were recorded on Perkin Elmer Ls55 Luminescence Spectrometer. Fluorescence spectra of solid powders were recorded in front-face geometry with 380 nm excitation wavelength. Fluorescence life time decay was recorded in a time-correlated single-photon-counting spectrometer of Horiba-Jobin Yvon. The fluorescent quantum yields were measured using an absolute photoluminescence quantum yield measurement system. Solid state ^{13}C NMR CPTOSS measurements were performed on Brucker Avance 400 (400 MHz) spectrometer with MAS rate of 5 kHz. Infrared (IR) spectra were recorded on small amount of the samples embedded in KBr pellets using a Bruker FT-IR spectrometer. Thermogravimetric analysis (TGA) was carried out (Mettler Toledo) in nitrogen atmosphere (flow rate 50 mLmin^{-1}) in the temperature range 30–600 ^{o}C (heating rate 5 ^{o}C/min). CHNS analyses were carried out using Thermo Scientific Flash 2000 Elemental Analyzer. Powder XRD pattern of the compounds were recorded by in Bruker D8 Discover (40 kV, 30 Ma) instrument using Cu Kα radiation (2θ = 0.8–60^{o}).

Computational details

The tetrabiphenyl pyrene monomer was optimized using Gaussian-09 suite of programs.[59–61] The optimization was carried out within Density Functional Theory (DFT) using B3LYP hybrid exchange-correlation functional and 6-31G basis set. The optimised geometries were visualised using Visual Molecular Dynamics (VMD).[62]

Adsorption measurements

N_2 gas adsorption study of the degassed samples (degassed at 210 °C for 18 h under vacuum) were carried out using QUANTACHROME QUADRASORB-*SI* analyzer at 77 K. The adsorbates were charged into the sample tube, and then the change of the pressure was monitored, the degree of adsorption was determined by the decrease of the pressure at the equilibrium state. All operations were computer-controlled and automatic.

Adsorption of toluene vapour at 293 K was measured for the desolvated **PY-BPP** using a BELSORP-aqua-3 analyzer. A sample of about ~ 100–150 mg was prepared by heating at 210 °C for about 18 h under vacuum (1×10^{-1} Pa) prior to measurement of the isotherms. The solvent used to generate the vapour was degassed fully by repeated evacuation. Dead volume was measured with helium gas. The adsorbate was placed into the sample tube, then the change of the pressure was monitored and the degree of adsorption was determined by the decrease in pressure at the equilibrium state. All operations were computer controlled and automatic.

Synthesis

Compounds TBP and BDPE were purchased from Aldrich.

Synthesis of Py-BPP:

A mixture of TBP (0.19 mmol) and 4,4′-Biphenyldiboronic acid bis(pinacol) ester (BDPE, 0.19 mmol) in DMF (20 mL) was degassed by four freeze-pump-thaw cycles. To this mixture 2M K_2CO_3 in water (2 mL) and tetrakis(triphenylphosphine)-palladium(0) (45 mg, 38.9 μmol) were added followed by degassing by four freeze-pump-thaw cycles. After that the resultant mixture was purged with Ar for 3 times and stirred at 130 °C in a schlenk flask for 36 h. After cooling to room

temperature the mixture was poured into water and filtered. The precipitate was washed with methanol, dichloromethane and dried in vacuum. The precipitate was further purified by soxhlet extractions with methanol, dichloromethane, toluene and tetrahydrofuran for 12 h each to give the product as a green solid (140 mg). **Py-BPP** polymer is practically insoluble in all common organic solvents and hence cannot be characterized using conventional methods of soluble polymers. Solid-state ^{13}C NMR (100 Mz, δ; ppm): 126.5, 132.7, 138.4; FT-IR (ν; cm^{-1}): 3025, 2913, 1602, 1485, 1359, 1145, 1095, 1004, 823, 728; Elemental Analysis (%) calculated for $C_{40}H_{22}$: C 95.617, H 4.383; found: C 89.47; H 4.42.

RESULTS AND DISCUSSION

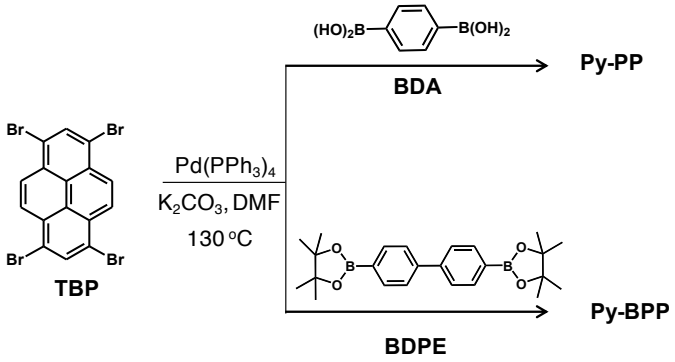

Scheme 2 Synthetic schemes for **Py-PP** and **Py-BPP**.

Synthesis, swelling and gas storage properties of **Py-PP** were previously reported by us.[31] **Py-BPP** is synthesized via Suzuki cross coupling reaction between 1,3,6,8-tetrabromopyrene (**TBP**) and 4,4′-Biphenyldiboronic acid bis(pinacol) ester (**BDPE**).[63] The topologies of these two polymers were first prepared by Jiang et al. using Yamamoto coupling which would give statistical copolymers.[64] However in the present case, Suzuki heterocoupling reactions ensures the perfectly alternating monomer sequence in the resulting polymer structures. As a result, the photophysical properties of these polymers would significantly vary depending on the syntheis conditions. The structure of **Py-BPP** characterized by solid-state ^{13}C-CP TOSS NMR, FT-IR and thermogravimetric analysis (TGA) (Scheme 2).[63] The appearence of two sets of peaks at 138-133 ppm, and 126.5 ppm, in ^{13}C-CP TOSS NMR corresponds to two types of unsubstituted and substituted phenyl carbon atoms respectively and hence consistennt with the proposed alternating structure of **Py-BPP**.[63] Presence of pyrene-phenylene linkages in the polymer backbone is also evident from the FT-IR measurements, which showed signals corresponding to aromatic C=C stretch (1595 cm^{-1}), C=C vibrational modes (1390 and 1480 cm^{-1}) of the substituted phenyl rings and aromatic C–H stretch (3030–3010 cm^{-1}).[63] **Py-BPP** failed to show any diffraction peaks due to its amorphous nature similar to several other organic microporous polymers.[63] The high thermal stability of **Py-BPP** was confirmed using thermogravimetric analysis (TGA).[63] TGA profile showed that **Py-BPP** is thermally stable up to 350 °C and the observed weight loss at the initial stages of heating (~200 °C) could be attributted to the trapped solvent molecules. Surface area and porosity of **Py-BPP** was evaluated using N_2 gas adsorption experiments at 77 K (Fig. 1a).[63] The activated polymer at 210 °C, showed a typical type-I profile isotherm with steep uptake at low pressure regions, symptomatic of the permanent microporous nature of the networks and the evaluated BET (Brunauer–Emmett–Teller) surface area is 350 m^2/g. The sudden increase in N_2 uptake at P/P_0 > 0.8 by the polymer is attributed to the interparticulate porosity associated with the meso- and macrostructures of the sample in the bulk.[63] We have also calculated the differential pore volume distributions for **Py-BPP** as a function of pore width calculated using the nonlocal DFT (NLDFT) method. **Py-BPP** have pore-size lessthan 25 Å indicating its microporous nature.[63] The BET surface area of **Py-PP** (1070 m^2/g) is much higher than **Py-BPP**. This clearly indicate that by judicious choice of linker, it is possible to tune the surface area, porosity and photophysical properties of the resultant polymers.[65,66] Interestingly, BET surface areas of the perfectly alternating polymers (**Py-PP** and **Py-BPP)** reported here closely match with statistical copolymers reported by Jiang et al.[64]

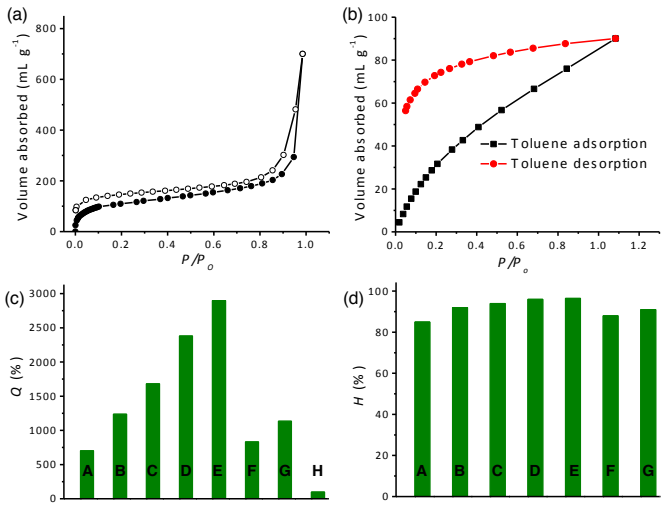

Fig. 1 (a) N_2 gas sorption isotherms (77 K) of the desolvated **Py-BPP** (closed symbols show the adsorption and open symbols show the desorption). (b) Toluene vapour adsorption isotherms of **Py-BPP** at 293 K; the sample was degassed at 483 K before measurement and the equilibrium time was 500 s. Swelling behaviour of **Py-BPP** expressed in terms of (c) Q (%) and (d) H (%), in various organic solvents with different polarities (A: hexane, B: diesel, C: toluene, D: ODCB, E: chloroform, F: ethanol , G: DMF, H:water).

Similar to previously reported **Py-PP**, the biphenyl bridged **Py-BPP** framework also exhibits dynamic behaviour as evidenced from the toluene vapour adsorption measurements (Fig. 1b). The rapid uptake of solvent by **Py-BPP** at low relative pressures (P/P_0 ~ 0.2) followed by a monotonic increase with pressure and ending without saturation at P/P_0 ~1 indicates the dynamic nature of **Py-BPP** framework. Moreover, the incomplete desorption along with large hysteresis indicates strong interaction of the toluene molecules with the pore surface of **Py-BPP**. We have further quantified the solvent uptake by **Py-BPP** in terms of their equilibrium state of

swelling parameter (Q%) and equilibrium solvent content (H%), that are calculated from the weight of dried and swollen polymers (Fig. 1c,d).[63] These parameters would reflect the ability of **Py-BPP** in absorbing various organic liquids under ambient conditions which is of practical relevance. For various organic solvents, the Q% and H% are varied between 900-3000 and 90-99 respectively, suggesting the superabsorbent nature of **Py-BPP**. Similar to **Py-PP**, **Py-BPP** also displayed high uptake for medium polar solvents like chloroform and *ortho*-dichlorobenzene (ODCB) than nonpolar (hexane) and polar (ethanol) solvents and failed to swell in water due to its hydrophobic nature. The differences in the amount of solvent uptake might also be dependent on the size and shape of the guest molecules and specific π-π interactions between host-guest components. This is quite remarkable property for **Py-PP** and **Py-BPP** polymers, compared to MOFs which cannot show superabsorbent nature for wide range of organic solvents.

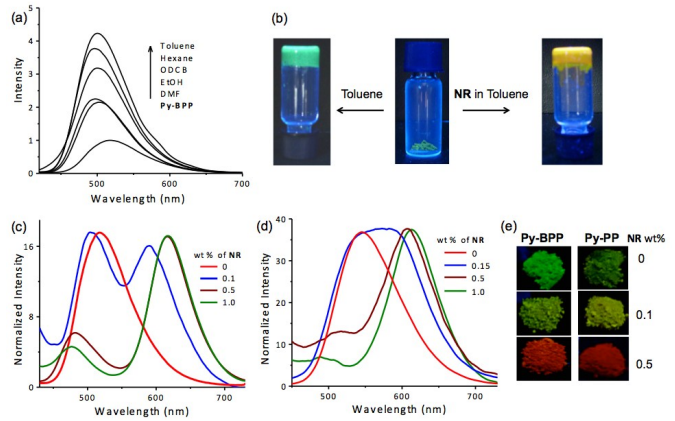

Fig. 2 (a) Fluorescence enhancement of **Py-BPP** after treatment with different organic solvents. (b) Photographs showing the swelling and gel formation by **Py-BPP** powder in toluene and toluene containing **NR** under 365 nm UV light. Normalized emission spectra of (c) **Py-BPP** and (d) **Py-PP** powders with different wt% of **NR** loading and their (e) corresponding photographs under 365 nm UV light.

Py-BPP exhibits green emission (470-650 nm) with a maximum at 517 nm (λ_{exc} = 380 nm). Similar to **Py-PP**, **Py-BPP** also displayed red-shifted absorption and emission compared to tetraphenyl pyrene chromophoric unit (λ_{abs} = 320 nm and λ_{em} = 450 nm),[67] due to the presence of extended conjugation in the polymer. The absorption spectra of both **Py-PP** and **Py-BPP** are approximately blue shifted by 30 nm compared to their corresponding statistical copolymers reported by Jiang et al.[31,64] However, in case of fluorescence properties, **Py-PP** emission closely matches with itsstatistical copolymer whereas **Py-BPP** show nearly 70 nm blue shift. These observations onceagin confirm that the photophysical properties of therese polymers are higly depend on the synthesis conditions. The swelling of **Py-BPP** in various organic solvents is accompanied by fluorescence enhancement indicating the guest induced structural changes in the conjugated backbones of the polymer (Fig. 2a). The soaked polymers in various solvents showed visible colour changes and bright green emission with an enhancement in fluorescence intensity with varying orders of magnitude depending on the solvent nature and polarity. Interestingly, self-standing fluorescent gels were formed when the polymer was soaked in toluene indicating their soft and superabsorbent nature (Fig. 2b). Additionally, the emission spectra of the solvent treated polymers were blue-shifted by 10-25 nm with respect to the desolvated samples probably due to unfolding of polymer backbones and reduced aggregation due to swelling. In the present case, fluorescence response of POPs towards organic solvents reiterates the dynamic nature of polymer framework. The maximum fluorescence enhancement (4-5 times) was observed for aromatic non-polar solvent like toluene whereas the polar solvents like ethanol showed only 2 times enhancement in the emission and did not show any fluorescence response with water, further proving the hydrophobic interior of the polymer. Hence emission changes with solvent molecules can be used as a probe to understand the swelling induced structual changes of **Py-BPP** framework.

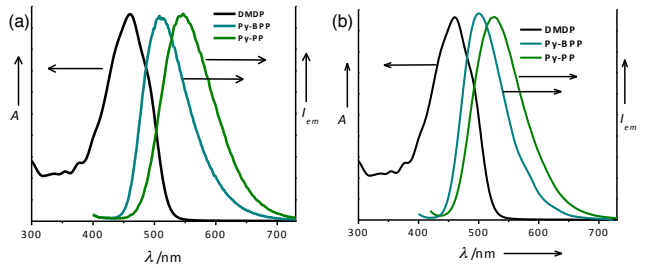

Fig. 3 Normalized absorption spectra of **DMDP** (in toluene) with the emission spectra of **Py-BPP** and **Py-PP** a) before, and b) after swelling in toluene.

We envisaged that the instantaneous swelling of both **Py-PP** and **Py-BPP** in various organic solvents and their hydrophobic interior would enable the simple and rapid encapsulation of luminescent hydrophobic dye molecules inside their pores. For this purpose, both polymers were swelled in toluene with different amounts of a well known hydrophobic dye, **NR** and dried under vacuum (Fig. 2b). Toluene was used as a mediating solvent for guest encapsulation due to good solubility of **NR** and excellent swelling behaviour of the polymers. Similar solution sate encapsulation was previously reported by Jiang et al. for the encapsulation of pyrene in the polypyrene porous network and the quenching the fluorescence of the host network was observed with increasing the amount of guest pyrene.[64] In the present study we took the advantage of swelling behaviour of our polymers for encapsulating photofunctional hydrophobic dyes for creating efficient light-harvesting antenna. Since our polymers exhibit a blue shift in their emission upon solvent guest encapsulation (*vide supra*), we expected similar fluorescence changes from the host frameworks as the **NR** is getting encapsulated. In contrast to organic solvents, the loading of **NR** led to the quenching in the emission of host frameworks with enhanced **NR** emission which could be due to energy transfer (*vide infra*) from host frameworks to the entrapped guest molecules (Fig. 2c,d). This further led to the tunable solid-state emission of both **Py-BPP** and **Py-PP** (Fig. 2e). However, residual emission of both the polymer networks after loading with **NR** was used as probe for guest

encapsulation. Remarkably, the residual emission of both polymers was gradually blue shifted with increasing wt% of **NR** in toluene suggesting its encapsulation inside the porous cavities of **Py-BPP** and **Py-PP** (*vide supra*, Fig. 2c,d). Initially a 13 nm blue shift in the emission of **Py-BPP** was observed with 0.1 wt% of **NR** loading which is further blue shifted to 36 nm with 0.5 wt% of **NR** and finally reached 40 nm with 1 wt% loading of **NR** (517 nm to 477 nm). Similarly, blue shifts up to 45 nm were observed in case of **Py-PP** emission with 1 wt% of loading **NR**. When **Py-BPP** treated with different solvents, maximum 15 nm blue shift was observed due to swelling. The observed large blue shifts in **NR** loaded polymers compared to the organic solvents is attributed to the large size of **NR** which would minimize aggregation of the backbone to a greater extent.

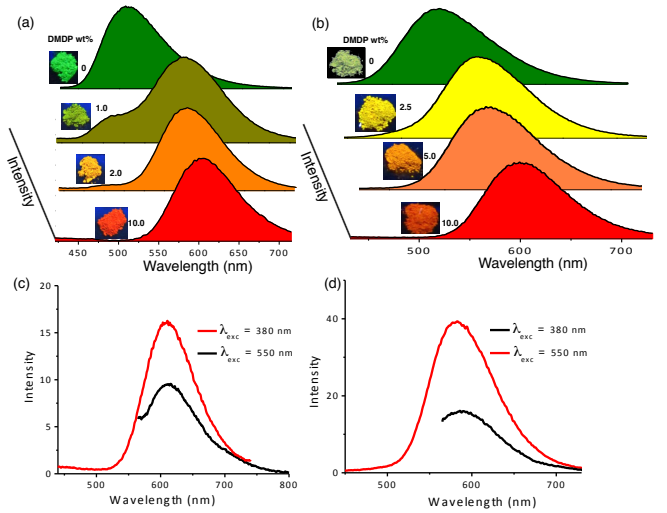

Fig. 4 Normalized emission spectra of (a) **Py-BPP** and (b) **Py-PP** loaded with different wt% of **DMDP.** Insets show the photographs of **Py-BPP** (inset of 4a) and **Py-PP** (inset of 4b) powders under 365 nm UV light loaded with different wt% of **DMDP** (fluorescence measurements were done with a front-face geometry, λ_{exc} = 380 nm). Emission spectra of directly (λ_{exc} = 380 nm) and indirectly (λ_{exc} = 500 nm) excited (c) **Py-BPP** loaded with 10.0 wt% and (d) **Py-PP** loaded with 2.5 wt% of **DMDP** dye.

The ability of these polymers to absorb wide variety of guest molecules, irrespective of their size highlights the role of dynamic porous framework as it can reorganize according to the incoming guest molecules. Moreover, the encapsulation of **NR** and tunable solid-state emission was further encouraged us to swell these polymers with appropriate luminescent acceptor molecules to facilitate efficient Förster type energy transfer (FRET) from the pyrene frameworks to the guest molecules. Though the energy transfer was shown in porous organic polymers,[52–54] encapsulation of guest requires overnight stirring at high temperatures which can be made easier with dynamic porous polymer. Since visible light-harvesting is preferred for many practical applications, we have used red emitting **DMDP** as the acceptor dye to harvest visible excitation energy from **Py-PP** and **Py-BPP**. In our case, the dynamic and swelling nature of these polymers allowed quick, controlled and room temperature encapsulation of **DMDP** dye. Encapsulation of **DMDP** was performed in similar way as **NR**, using toluene as a mediating solvent. In a typical experimental procedure different amounts of dye were dissolved in 0.5 mL toluene and added to 30 mg of polymers. The resultant swelled polymer-dye composites were kept at room temperature for 30 min and dried at room temperature as well as in vacuum to remove the toluene, completely. The resultant powders loaded with different wt% of **DMDP** were used for optical measurements. The gradual ground state colour and excited state luminescence changes in the polymer powders with increasing guest loading further confirm their encapsulation within the porous cavities of the polymers.

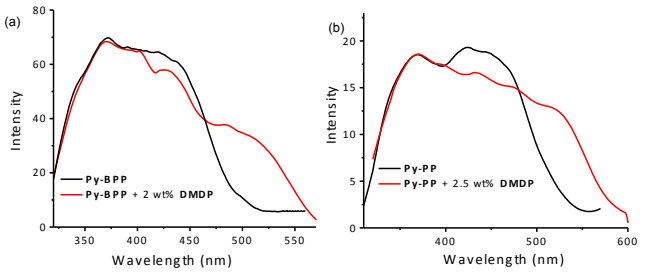

Fig. 5 Excitation spectra of (a) **Py-BPP** powder with (monitored at 650) and without (monitored at 540) **DMDP**. Excitation spectra of (b) **Py-PP** powder with (monitored at 650) and without (monitored at 560) **DMDP**.

The good spectral overlap between emission of **Py-BPP** and **Py-PP** polymer powders with the absorption spectrum of **DMDP** dye indicates that it would be possible to make efficient light-harvesting antenna from these host-guest molecules (Fig. 3). Energy transfer experiments were performed with varying amounts of **DMDP** loading (0-10 wt%) inside the porous network of the polymers. As the amount of encapsulated **DMDP** increases, gradual quenching in the emission of both the donor frameworks with concomitant increase in the **DMDP** emission (600-700 nm) intensity was observed (Fig. 4a,b).[63] This gives an indication of excitation energy transfer from host frameworks (**Py-BPP** and **Py-PP**) to the entrapped dye molecules. To show the encapsulation of dye molecule we have measured the surface area before and after encapsulation of 10 wt% **DMDP** dye.[63] However, in order to evaluate the surface area we had to degas the dye containing polymers at high temperature (**210 °C**) and high vacuum (**10^{-1} Pa**). Under such harsh conditions the incorporated dye molecules can decompose or can come out of the pores. This could be reason why we are not seeing significant decrease in the micropore step.[63] Alternatively, we showed that fluorescence could be used to prove the dye encapsulation. When solvent molecules are incorporated we see the blue shift in the fluorescence maximum of polymer (*vide supra*). Similar blue shift in the fluorescence (**up to ~ 45 nm**) maximum of polymer was observed after dye incorporation (Fig. 4a). This convincingly support the encapsulation of dye molecules in the micropores of the polymer. Moreover, the absence of vibronic features in the **DMDP** emission when it was loaded into the pores of **Py-BPP** and **Py-PP** confirms the existence of orientational dipolar interactions between **DMDP** and aromatic shells of host frameworks.[68] These kinds of dipolar interactions are indeed important to achieve efficient Förster

type energy transfer between donor and acceptor chromophores. This inherent property of **DMDP** to show orientational dipolar interactions[68] with aromatic and polar solvents is an added advantage in addition to the dynamic behaviour of **Py-BPP** and **Py-PP** in the construction of present visible light-harvesting antenna. In these host-guest systems, 2.0-2.5 wt% of guest was able to completely harvest the excitation energy from host frameworks indicating efficient energy-transfer process. The observed gradual red-shift in the emission maxima of encapsulated **DMDP** molecules (up to 30 nm) with increasing its concentration are attributed to the formation of **DMDP** aggregates inside the pores at higher amounts of loading (~10 wt%).[58] Emission spectra, collected for different wt% of **DMDP** loaded polymers indicates that, at below 2 wt% of **DMDP** energy-transfer is mainly to its isolated species (**DMDP**, λ_{max} = 570 nm), where all **DMDP** molecules are spatially distributed inside the pore channels. On the other hand, above 2 wt% of **DMDP** loading, energy-transfer happens mostly to its aggregated species (λ_{max} = 604 nm). This was further rationalized by the observed amplified fluorescence of **DMDP** by energy-transfer in this host-guest system (Fig. 4c,d). In case of **Py-BPP** loaded with 10 wt% of the **DMDP**, excitation at 380 nm (indirect excitation) results in nearly 2 times higher **DMDP** emission due to energy-transfer, compared to its direct excitation at 550 nm. Similarly 2.5 times amplification in the **DMDP** emission was observed in case of **Py-PP** loaded with 2.5 wt% of **DMDP**. This clearly indicates that the enhancement in the emission of both isolated and aggregated **DMDP** molecules inside the pores is indeed due to efficient resonance energy-transfer from host framework to the entrapped guest molecules. Furthermore, the controlled loading of **DMDP** molecules inside the polymers leads to the tunable emission from green to yellow to red. This is visually shown in the photographs taken under 365 nm UV-irradiation of **Py-BPP** and **Py-PP** powders loaded with different wt% of **DMDP** (insets, Fig. 4a,b). As shown in the insets of Fig. 4a, **Py-BPP** alone is green emissive, with 1 wt% of **DMDP** loading leads to greenish yellow, at 2 wt% it is yellow and finally at 10 wt% the polymer is orange-red emissive. Similar colour trends were seen in case of **Py-PP** loaded with different wt% of **DMDP** (Fig. 4b). Energy-transfer in these host-guest antenna materials was confirmed by excitation spectra collected at both polymers (host) and **DMDP** (guest) emission wavelengths (Fig. 5). The appearance of absorption features of both polymer and **DMDP** in the excitation spectra collected for both **Py-BPP- DMDP** and **Py-BPP- DMDP** host-guest systems at **DMDP** emission (650 nm) wavelength, where polymers have negligible emission, unambiguously supports the population of **DMDP** excited states via energy-transfer from host polymers.

Further investigations on fluorescence lifetime and absolute quantum yields of these host-guest antenna materials provided decisive proof for the resonance energy transfer from host frameworks to the guest molecules without any radiation reabsorption process (Fig. 6). The lifetime decay profiles were fitted with triexponentials and average lifetime was considered for the analyses. **Py-BPP** framework with an average lifetime of 2.49 ns in its solid state, decreased to 2.1 ns (monitored at 500 nm) after loading with 2 wt% of **DMDP**. Similarly, the average lifetime of **Py-PP** also shortened from 0.72 ns to 0.58 ns (monitored at 520 nm) with 2.5 wt% of **DMDP** loading. This decrease in the excited state lifetimes of host frameworks upon encapsulation of **DMDP** is a clear indication of excited state energy-transfer mechanism for fluorescence quenching of host frameworks. Absolute quantum yield measurements further gave quantitative picture for the efficiency of energy transfer process. The high absolute quantum yield (ϕ = 0.56%) of **DMDP** (2 wt%) loaded **Py-BPP** compared to the individual **Py-BPP**(ϕ = 0.31%) and **DMDP** (ϕ = 0.24%) indicates efficient resonance energy transfer without any radiation reabsorption process.

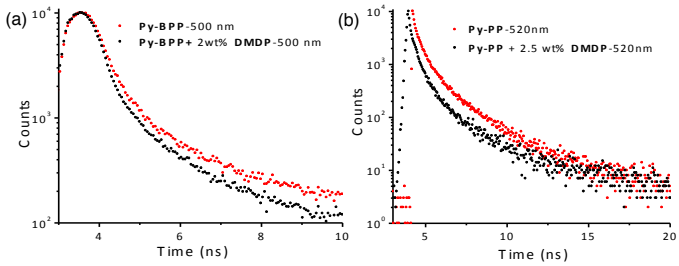

Fig. 6 Lifetime decay profiles of (a) **Py-BPP** and (b) **Py-PP** alone and with **DMDP** (lifetime measurements were done with a front-face geometry, λ_{exc} = 380 nm). Wavelengths in graphs indicate the where decay profiles were monitored.

Conclusions

In conclusion this work introduces a novel class of multi-functional conjugated organic microporous polymers, in which the porous fluorescent frameworks can undergo structural reorganization in presence of hydrophobic and aromatic guest molecules. This further imparted unprecedented properties, such as super-absorbency and swelling in these polymers. The dynamic nature of these porous polymeric frameworks enabled facile encapsulation of guest molecules. Furthermore, the fluorescent pyrene scaffold combined with the dynamic porosity facilitated guest-induced emission changes and encapsulation of luminescent hydrophobic guests led to the tunable solid-state emission via light-harvesting. The unique ability of these polymers to encapsulate various guest molecules with fluorescence response behaviour holds a great promise in designing smart materials from simple building blocks for sensing, separation and photocatalysis.

Acknowledgements

We thank Prof. C. N. R. Rao for his support and encouragement. We thank JNCASR and DST for financial support. We thank Prof. S. Balasubramanian and C. Kulkarni for the computational experiments. K.V.R. and R.H. thank CSIR for a research fellowship.

Notes and references

1 P. D. Frischmann and M. J. MacLachlan, *Chem. Soc. Rev*., 2013, **42**, 871–890.
2 R. N. Dsouza, U. Pischel and W. M. Nau, *Chem. Rev.*, 2011, **111**, 7941–7980.
3 H. Amouri, C. Desmarets and J. Moussa, *Chem. Rev.*, 2012, **112**, 2015–2041.
4 K. Tashiro and T. Aida, *Chem. Soc. Rev.*, 2007, **36**, 189–197.
5 Z. Laughreya and B. C. Gibb, *Chem. Soc. Rev.*, 2011, **40**, 363–386.
6 R. Joseph and C. P. Rao, *Chem. Rev.*, 2011, **111**, 4658–4702.
7 J. Jr. Rebek, *Acc. Chem. Res.*, 2009, **42**, 1660–1668.
8 M. Yoshizawa, J. K. Klosterman, and M. Fujita, *Angew. Chem. Int. Ed.*, 2009, **48**, 3418–3438.
9 Y. Inokuma, M. Kawano and M. Fujita, *Nat. Chem*., 2011, **3**, 349–358.
10 S. Kitagawa, R. Kitaura and S.-i. Noro, *Angew. Chem. Int. Ed.*, 2004, **43**, 2334–2375.
11 J.-P. Zhang, Y.-B. Zhang, J.-B. Lin and X.-M. Chen, *Chem. Rev.*, 2012, **112**, 1001–1033.
12 N. Mizoshita, T. Taniab and S. Inagaki, *Chem. Soc. Rev.*, 2011, **40***,* 789–800.
13 B. V. V. S. P. Kumar, K. V. Rao, T. Soumya, S. J. George and M. Eswaramoorty, *J. Am. Chem. Soc.*, 2013, **135***,* 10902–10905.
14 B. V. V. S. P. Kumar, K. V. Rao, S. Sampath, S. J. George and M. Eswaramoorty, *Angew. Chem. Int. Ed*., 2014, **53**, 13073–13077.
15 L. M. Lanni, R. W. Tilford, M. Bharathy and J. J. Lavigne, *J. Am. Chem. Soc.*, 2011, **133**, 13975–13983.
16 Y. Du, K. Mao, P. Kamakoti, P. Ravikovitch, C. Paur, S. Cundy, Q. Li and D. Calabro, *Chem. Commun.*, 2012, **48**, 4606–4608.
17 Y. Inokuma, T. Arai and M. Fujita, *Nat. Chem*., 2010, **2**, 780–783.
18 A. I. Cooper, *Adv. Mater*., 2009, **21**, 1291–1295; Z. Chang, D.-S. Zhang, Q. Chen and X.-H. Bu, *Phys. Chem. Chem. Phys*., 2013,**15**, 5430-5442; Y. Li, S. Roy, T. Ben, S. Xu and S. Qiu, *Phys. Chem. Chem. Phys.*, 2014,**16**, 12909-12917.
19 J.-X. Jiang, F. Su, C. D. Wood, N. L. Campbell, H. Niu, C. Dickinson, A. Y. Ganin, M. J. Rosseinsky, Y. Z. Khimyak, A. I. Cooper and A. Trewin, *Angew. Chem., Int. Ed*., 2007, **46**, 8574–8578.
20 J. Weber and A. Thomas, *J. Am. Chem. Soc*., 2008, **130**, 6334–6335.
21 P. Kuhn, M. Antonietti and A. Thomas, *Angew. Chem. Int. Ed*., 2008, **47**, 3450–3453.
22 T. Ben, H. Ren, S. Ma, D. Cao, J. Lan, X. Jing, W. Wang, J. Xu, F. Deng, J. M. Simmons, S. Qiu and G. Zhu, *Angew. Chem. Int. Ed*., 2009, **48**, 9457–9460.
23 L. Chen, Y. Yang, Z. Guo, and D. Jiang, *Adv. Mater*., 2011, **23**, 3149–3154.
24 K. V. Rao, S. Mohapatra, C. Kulkarni, T. K. Maji and S. J. George, *J. Mater. Chem*., 2011, **21**, 12958–12963.
25 A. P. Katsoulidis and M. G. Kanatzidis, *Chem. Mater.*, 2011, **23**, 1818–1824.
26 K. V. Rao, R. Haldar, C. Kulkarni, T. K. Maji and S. J. George, *Chem. Mater.*, 2012, **24**, 969−971.
27 K. V. Rao, R. Haldar, C. Kulkarni, T. K. Maji and S. J. George, *Polymer*, 2014, **55**, 1452–1458.
28 S. Kitagawa and K. Uemura, *Chem. Soc. Rev*., 2005, **34**, 109–119.
29 T. K. Maji, K. Uemura, H.-C. Chang, R. Matsuda and S. Kitagawa, *Angew. Chem. Int. Ed.*, 2004, **43**, 3269–3272.
30 N. Yanai, K. Kitayama, Y. Hijikata, H. Sato, R. Matsuda, Y. Kubota, M. Takata, M. Mizuno, T. Uemura and S. Kitagawa, *Nat. Mater.*, 2011, **10**, 787–793.
31 K. V. Rao, S. Mohapatra, C. Kulkarni, T. K. Maji and S. J. George, *Chem. Eur. J.*, 2012, **18**, 4505–4509.
32 X. Liu, Y. Xu, Z. Guo, A. Nagai and D. Jiang, *Chem. Commun.*, 2013, **49**, 3233–3235.
33 X. Liu, Y. Xu and D. Jiang, *J. Am. Chem. Soc.*, 2012, **134**, 8738–8741.
34 R. S. Sprick, J.-X. Jiang, B. Bonillo, S. Ren, T. Ratvijitvech, P. Guiglion, M. A. Zwijnenburg, D. J. Adams and A. I. Cooper, *J. Am. Chem. Soc*., 2015, **137**, 3265–3270
35 M. D. Ward, *Chem. Soc. Rev*., 1997, **26**, 365–375.
36 A. Ajayaghosh, V. K. Praveen and C. Vijayakumar, *Chem. Soc. Rev*., 2008, **37**, 109–122; A. Ajayaghosh, S. J. George and V. K. Praveen, *Angew. Chem. Int. Ed*., 2003, **42**, 332–335; C. Vijayakumar, V. K Praveen and A. Ajayaghosh, *Adv. Mater*., 2009, **21**, 2059–2063; C. Vijayakumar, V. K. Praveen, K. K. Kartha and A. Ajayaghosh, *Phys. Chem. Chem. Phys.*, 2011,**13**, 4942–4949.
37 P. D. Frischmann, K. Mahata and F. Würthner, *Chem. Soc. Rev.*, 2013, **42**, 1847–1870.
38 S. Inagaki, O. Ohtani, Y. Goto, K. Okamoto, M. Ikai, K. Yamanaka, T. Tani and T. Okada, *Angew. Chem. Int. Ed*., 2009, **48**, 4042–4046.
39 K. V. Rao, K. K. R. Datta, M. Eswaramoorty and S. J. George, *Angew. Chem. Int. Ed*., 2011, **50**, 1179–1184.
40 S. S. Babu, K. K. Kartha and A. Ajayaghosh, *J. Phys. Chem. Lett*., 2010, **1**, 3413–3424.
41 K. V. Rao, K. K. R. Datta, M. Eswaramoorthy and S. J. George, *Adv. Mater.* 2013, **25**, 1713−1718.
42 K. V. Rao, K. K. R. Datta, M. Eswaramoorthy and S. J. George, *Chem. Eur. J.*, 2012, **18**, 2184−2194.
43 K. V. Rao, A. Jain and S. J. George, *J. Mater. Chem.* C, 2014, **2**, 3055−3064.
44 X. Zhang, M. A. Ballem, Z.-J. Hu, P. Bergman and K. Uvdal, *Angew. Chem. Int. Ed.*, 2011, **50,** 5729–5733.
45 X. Zhang, M. A. Ballem, M. Ahrén, A. Suska, P. Bergman and K. Uvdal, *J. Am. Chem. Soc.*, 2010, **132**, 10391–10397.
46 X. Zhang, Z.-K. Chen and K. P. Loh, *J. Am. Chem. Soc.*, 2009, **131**, 7210–7211.
47 C. Y. Lee, O. K. Farha, B. J. Hong, A. A. Sarjeant, S. T. Nguyen and J. T. Hupp, *J. Am. Chem. Soc.*, 2011, **133**, 15858–15861.
48 R. Haldar, K. V. Rao, S. J. George and T. K. Maji, *Chem. Eur. J.*, 2012, **19**, 5848–5852.
49 R. Haldar, R. Matsuda, S. Kitagawa, S. J. George and T. K. Maji, *Angew. Chem. Int. Ed.*, 2014, **53**, 11772–11777.
50 M. V. Suresh, S. J. George and T. K. Maji, *Adv. Funct. Mater.*, 2013, **23**, 5585–5590.
51 N. Mizoshita, Y. Goto, Y. Maegawa, T. Tani and S. Inagaki, *Chem. Mater.*, 2010, **22**, 2548–2554.
52 L. Chen, Y. Honsho, S. Seki and D. Jiang, *J. Am. Chem. Soc*., 2010, **132**, 6742–6748.
53 A. Patra and U. Scherf, *Chem. Eur. J.*, 2012, **18**, 10074–10080.
54 V. M. Suresh, S. Bonakala, S. Roy, S. Balasubramanian and T. K. Maji, *J. Phys. Chem. C*, 2014, **118**, 24369–24376.
55 L. Chen, Y. Yang and D. Jiang, *J. Am. Chem. Soc.*, 2010, **132**, 9138–9143.
56 Y. Xu, L. Chen, Z. Guo, A. Nagai and D. Jiang, *J. Am. Chem. Soc.* 2011, **133**, 17622–17625.
57 Y. Xu, A. Nagai and D. Jiang, *Chem. Commun.* **2013**, *49*, 1591–1593.
58 A. Ajayaghosh, C. Vijayakumar, V. K. Praveen, S. S. Babu and R. Varghese, *J. Am. Chem. Soc.*, 2006, **128**, 7174–7175.
59 M. J. Frisch *et al., Gaussian, Inc. Wallingford CT*, 2010.
60 A. D. Becke, *J. Chem. Phys.* **1993**, *98*, 5648–5652.
61 C. Lee, W. Yang and R. G. Parr, *Phys. Rev. B*, 1988, **37**, 785–789.
62 W. Humphrey, A. Dalke and K. Schulten, *J. Molec. Graphics*, 1996, **14**, 33–38.
63 See supporting information
64 J.-X. Jiang, A. Trewin, D. J. Adams and A. I. Cooper, *Chem. Sci*., 2011, **2**, 1777–1781.

65 J.-X. Jiang, F. Su, A. Trewin, C. D. Wood, H. Niu, J. T. A. Jones, Y. Z. Khimyak and A. I. Cooper, *J. Am. Chem. Soc.*, 2008, **130**, 7710–7720.
66 J.-X. Jiang, A. Trewin, F. B. Su, C. D. Wood, H. J. Niu, J. T. A. Jones, Y. Z. Khimyak and A. I. Cooper, *Macromolecules*, 2009, **42**, 2658–2666.
67 T. Oyamada, S. Akiyama, M. Yahiro, M. Saigou, M. Shiro, H. Sasabe and C. Adachi, *Chem. Phys. Lett*., 2006, **421**, 295–299.
68 S. L. Bondarev, V. N. Knyukshto, V. I. Stepuro, A. P. Stupak and A. A. Turban, *J. Appl. Spectros*co., 2004, **71**, 194–201.